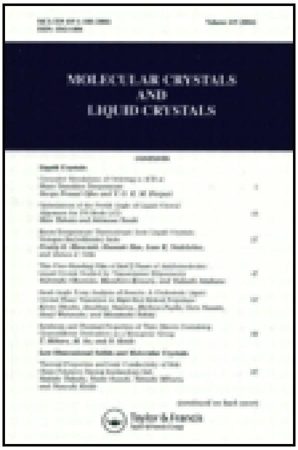

Molecular Crystals and Liquid Crystals
Publication details, including instructions for authors and subscription information:
http://www.tandfonline.com/loi/gmcl20

Carrier Transport Mechanisms in Organic Light-Emitting Devices with a N,N′-diphenyl-N,N′-bis(1-naphthyl)-1,1′-biphenyl-4,4′-diamine:tris-(8-hydroxyquinoline) Aluminum Mixed Layer Acting as an Emitting Layer

Y. B. Yoon [a], D. C. Choo [a], D. U. Lee [a], T. W. Kim [a], K. D. Kwack [a], J. H. Kim [b], J. H. Seo [c] & Y. K. Kim [c]

[a] Research Institute of Information Display, Division of Electronics and Computer Engineering, Hanyang University, Seoul, Korea

[b] Department of Electronic Engineering, Hong-ik University, Seoul, Korea

[c] Department of Information Display Engineering & COMID, Hong-ik University, Seoul, Korea

Version of record first published: 21 Dec 2006

To cite this article: Y. B. Yoon, D. C. Choo, D. U. Lee, T. W. Kim, K. D. Kwack, J. H. Kim, J. H. Seo & Y. K. Kim (2006): Carrier Transport Mechanisms in Organic Light-Emitting Devices with a N,N′-diphenyl-N,N′-bis(1-naphthyl)-1,1′-biphenyl-4,4′-diamine:tris-(8-hydroxyquinoline) Aluminum Mixed Layer Acting as an Emitting Layer, Molecular Crystals and Liquid Crystals, 458:1, 273-279

To link to this article: http://dx.doi.org/10.1080/15421400600932173

Mol. Cryst. Liq. Cryst., Vol. 458, pp. 273–279, 2006
Copyright © Taylor & Francis Group, LLC
ISSN: 1542-1406 print/1563-5287 online
DOI: 10.1080/15421400600932173

Taylor & Francis
Taylor & Francis Group

Carrier Transport Mechanisms in Organic Light-Emitting Devices with a N,N′-diphenyl-N,N′-bis(1-naphthyl)-1,1′-biphenyl-4,4′-diamine:tris-(8-hydroxyquinoline) Aluminum Mixed Layer Acting as an Emitting Layer

Y. B. Yoon
D. C. Choo
D. U. Lee
T. W. Kim
K. D. Kwack
Research Institute of Information Display, Division of Electronics and Computer Engineering, Hanyang University, Seoul, Korea

J. H. Kim
Department of Electronic Engineering, Hong-ik University, Seoul, Korea

J. H. Seo
Y. K. Kim
Department of Information Display Engineering & COMID, Hong-ik University, Seoul, Korea

The current density-voltage (J-V) measurements on organic light-emitting devices (OLEDs) with and without a N,N′-diphenyl-N,N′-bis(1-naphthyl)-1,1′-biphenyl-4,4′-diamine (NPB):tris-(8-hydroxyquinoline) aluminum (Alq_3) mixed layer were performed to investigate the carrier transport mechanism. The slopes of the double logarithmic J-V curves for the OLEDs with and without the mixed layer in the space-charge-limited current (SCLC) region were 6.5 and 2, respectively. The dramatic increase in the slope of the double logarithmic J-V curve for the OLEDs with the mixed layer was attributed to the decrease in the mobility difference of the charge carriers at the NPB/Alq_3 heterointerface resulting from the minimization of the energy barriers, and the carrier transport behaviors in the SCLC region were significantly affected by the unintentional virtual electrode, serving as a charge carrier reservoir, that formed at the heterointerface.

This work was supported by the Korea Research Foundation Grant funded by the Korean Government (MOEHRD Basic Research Promotion Fund) (KRF-2004-015-D00166).

Address correspondence to T. W. Kim, Research Institute of Information Display, Division of Electronics and Computer Engineering, Hanyang University, Seoul 133-791, Korea. E-mail: twk@hanyang.ac.kr

Keywords: carrier transport mechanism; mixed layer; organic light-emitting devices

PACS Numbers: 78.60. Fi and 78.66. Qn

I. INTRODUCTION

Organic light-emitting devices (OLEDs) have emerged as promising candidates for potential applications in the fabrication of full-color flat-panel displays with high efficiencies because they have the unique advantages of fast response, low power consumption, wide-view angle, high contrast, and large flexibility [1–5]. In spite of the several advantages of OLEDs in applications to flat-panel displays, OLEDs still have inherent problems due to limited self-luminescence [6,7], short lifetime [8,9], and poor color stability [10]. Since the local fields generated by the accumulated charges, the positive immobile charges, and the trapped charges in the space-charge-limited-current (SCLC) region degrade the efficiencies of the OLEDs, correlated studies between the electrical properties and the carrier transport mechanisms in OLEDs are necessary for improving the lifetimes of OLEDs. Even though many structural works concerning the enhancement of the efficiencies and the lifetimes of OLEDs utilizing various structures, such as a doped layer in the host mixed structure [11], a graded mixed structure [12], a fuzzy-junction structure [13], a multiple-quantum-well structure [14], an organic-inorganic hybrid structure [15], and a stacked structure [16], have been performed, studies on carrier transport mechanisms in OLEDs with a mixed layer acting as an emitting layer (EML) have not yet been carried out. Furthermore, systematic studies of the carrier transport mechanisms in OLEDs with a mixed layer acting as an EML play a very important role in enhancing the lifetimes of OLEDs.

This paper reports on the carrier transport mechanisms in OLEDs utilizing a mixed layers, acting as an EML, deposited by using organic molecular-beam deposition (OMBD). Current density-voltage (J-V) measurements were carried out to investigate electrical properties of the OLEDs with a mixed layer. The double logarithmic J-V characteristics of the OLEDs with and without a mixed layer were carried out to investigate the carrier transport mechanisms in the OLEDs.

II. EXPERIMENTAL DETAILS

The sheet resistivity and the thickness of the indium-tin-oxide (ITO) thin films coated on glass substrates used in this study were

30 Ω/square and 1000 Å, respectively. The ITO substrates were cleaned using sonications of acetone, methanol, and distilled water at 60°C for 15 min. The chemically cleaned ITO substrates were kept for 48 h in isopropyl alcohol. After the cleaned ITO substrates had been dried by using N_2 gas with a purity of 99.9999%, the surfaces of the ITO substrates were treated with an oxygen plasma for 2 min at an O_2 pressure of approximately 2×10^{-2} Torr. The three kinds of samples used in this experiment consisted of the following structures from the top: an aluminum (Al) cathode electrode, a lithium quinolate (Liq) electron injection layer (EIL), a tris-(8-hydroxyquinoline) aluminum (Alq_3) EML/electron transport layer (ETL) with a perylene, 4-dicyano-methylene-2-methyl-6–4-dimethylami-nostyryl-4H-piran (DCM1) as a yellow dopant (1%) [17], a N,N′-diphenyl-N,N′-bis(1-napthyl)-1,1′-biphenyl-4,4′-diamine (NPB) hole transport layer (HTL), an ITO anode electrode, and glass substrates. The doping concentration of DCM1 in the Alq_3 EML or the host mixed layer was 1% and was controlled by using the deposition rate. While the thicknesses of the Alq_3 layer and the NPB layer for the OLEDs were different, the distance from the Al cathode to the DCM1 dopant interface for electron injection was maintained at a constant value of 50 nm. After organic and metal depositions, the OLED devices were encapsulated in a glove box with O_2 and H_2O concentrations below 1 ppm. The organic materials were evaporated onto an ITO-coated glass substrate at a chamber pressure of about 3×10^{-6} Torr. The growth rates of the organic layers and the metal layers were approximately 0.01 Å/s and 1 Å/s, respectively.

The J-V characteristics of the OLEDs were measured on a programmable electrometer with built-in current and voltage measurement

TABLE 1 OLEDs with Various Structures Used in this Study. The Mixed Layer Consists of NPB and Alq_3, and the Ratio of the Deposition Rate of the NPB Layer to that of the Alq_3 Layer is 1:1. The Doping Concentration of the DCM1 Molecule in the Emitting Layer is 1%

Device Layer	I	II	III
Anode		Al	
EIL (nm)		Liq (2)	
ETL (nm)	Alq_3 (60)	Alq_3 (50)	Alq_3 (50)
EML:DCM1 (nm)		Alq_3 (10)	Mixed NPB:Alq_3 (10)
HTL (nm)		NPB (50)	
Cathode		ITO	

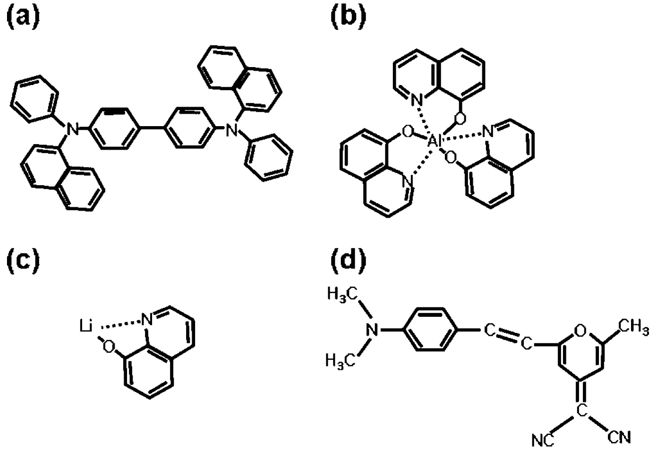

FIGURE 1 Molecular structures of the organic layers used in this study: (a) NPB, (b) Alq_3, (c) Liq, (d) DCM1.

units (MODEL 236, Keithely). The brightness was measured using a brightness meter (chroma meter CS-100A, Minolta). The OLED structures used in this study are summarized in Table 1, and the molecular structures of the organic layers used in this study are shown in Figure 1. Schematic energy band diagrams of the fabricated OLEDs with various structures used in this study are shown in Figure 2.

III. RESULTS AND DISCUSSION

The J-V characteristics of the OLEDs with various structures show that the current density of device III is smaller than those of devices I and II at the same driving voltage, which is attributed to an increase in trap states generated by the dopant DCM1 and the host NPB

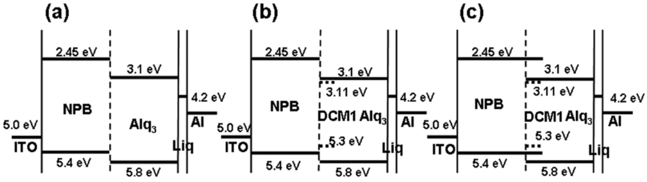

FIGURE 2 Schematic energy diagrams of devices (a) I, (b) II, and III. The LUMO and the HOMO represent the lowest unoccupied molecular orbital and the highest occupied molecular orbital, respectively, and the energy level of 0 eV indicates a vacuum level.

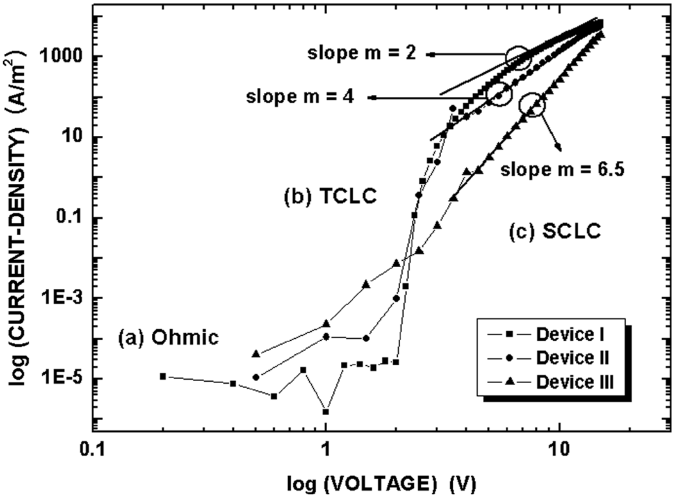

FIGURE 3 Double logarithmic plot of the current density-voltage for the OLEDs with various structures.

resulting from the existence of the DCM1 doped NPB:Alq$_3$ mixed layer in device III. Since the NPB and the DCM1 molecules coexist in the EML of device III, the increase in the operating voltage to achieve the same current density in device III is larger than those in devices I and II. Since the DCM1 and the NPB molecules in the mixed layer act as traps, which impede the charge transport and increase the hopping distances of the holes and the electrons, the significant variation in the carrier mobility in the layer can be removed by using a NPB:Alq$_3$ mixed layer.

The double logarithmic J-V characteristics of the OLEDs with various structures are shown in Figure 3. The double logarithmic J-V characteristics show that ohmic, trap-charge-limited current (TCLC), and the SCLC regions sequentially appear with increasing applied voltage and that the slopes of the double logarithmic J-V curves, which are given by $m = \Delta(\log J)/\Delta(\log V)$, are different for the three regions. When the TCLC density with an exponential trap distribution in the energy gap is determined from the trap distribution for electron injection [18], since the J-V characteristics exhibits a power law dependence of $J \propto V^{m+1}$, which is attributed to the continuous charging of exponential trap states, the TCLC region appears at the double logarithmic J-V characteristics of the OLEDs with various structures. A large injection into an organic layer with a low carrier mobility caused charge to be accumulated, which partially decreases the magnitude of the applied electric field, resulting in a redistribution of the charge. Since the carrier mobility in the SCLC region is independent of the electric field, the current density in the SCLC region obeys the Mott-Gurney equation [19,20].

The slope m of the double logarithmic J-V curve in the SCLC region under an applied electric field can be determined from the internal electric field and the screening effect due to the space charges existing at the organic heterointerfaces. Even though the theoretical slope of typical OLEDs operating in the SCLC region is 2, the slopes of devices II and III in the SCLC region are 4 and 6.5, respectively. The dramatic increase in the slope of the double logarithmic J-V curve for device III is attributed to the decrease in the mobility difference of the charge carriers at the NPB/Alq_3 heterointerface resulting from the minimization of the energy barriers. The holes injected from the anode to the organic layer in devices I and II accumulated at the organic heterointerface due to the existence of the energy barrier (0.4 eV) resulting from the difference between the highest occupied molecular orbital levels of the NPB and the Alq_3 layers, as shown in Figure 2. [21]. Therefore, an unintentional virtual electrode serving as a charge carrier reservoir was formed in the devices I and II, resulting in a lower slope in the SCLC region at a high applied electric field. The probability of a electron and a hole coexisting in the NPB:Alq_3 mixed layer in device III is relatively high, and the lowering of the heterointerface barrier due to the existence of the mixed layer increases the carrier transport. Since the carrier transport behaviors of the OLED device with a mixed layer are not significantly affected by a low density of space charges with $m = 6.5$, the space-charge distribution and the induced internal electric field at the NPB/Alq_3 heterointerface, together with the variations in the carrier distribution and the electric field under an applied voltage, are very important for understanding the carrier transport mechanism and for enhancing the long-time stability of OLEDs.

IV. SUMMARY AND CONCLUSIONS

The slopes of the double logarithmic J-V curves for the OLEDs with and without the mixed layer in the space-charge-limited current (SCLC) region were 6.5 and 2, respectively. The dramatic increase in the slope of the double logarithmic J-V curve for the OLEDs with the mixed layer was attributed to the decrease in the mobility difference of the charge carriers at the NPB/Alq_3 heterointerface resulting from the minimization of the energy barriers, and the carrier transport behaviors in the SCLC region were significantly affected by an unintentional virtual electrode, serving as a charge carrier reservoir, that formed at the heterointerface. These results can help improve understanding of carrier transport mechanisms in OLEDs with a mixed layer acting as an EML.

REFERENCES

[1] Chuen, C. H. & Tao, Y. T. (2002). *Appl. Phys. Lett.*, *81*, 4499.
[2] Wong, F. L., Fung, M. K., Jiang, X., Lee, C. S., & Lee, S. T. (2004). *Thin Solid Films*, *446*, 143.
[3] Yang, C.-J., Lin, C.-L., Wu, C.-C., Yeh, Y.-H., Cheng, C.-C., Kuo, Y.-H., & Chen, T.-H. (2005). *Appl. Phys. Lett.*, *87*, 143507.
[4] Kanno, H., Sun, Y., & Forrest, S. R. (2005). *Appl. Phys. Lett.*, *86*, 263502.
[5] Lewis, J., Grego, S., Chalamala, B., Vick, E., & Temple, D. (2004). *Appl. Phys. Lett.*, *85*, 3450.
[6] Chan, L., Yeh, H., & Chen, C. (2001). *Adv. Mater.*, *13*, 1637.
[7] Kohler, A., Wilcon, J. S., & Friend, R. H. (2002). *Adv. Mater.*, *14*, 701.
[8] Popovic, Z. D. & Aziz, H. (2002). *IEEE J. Selected Topics in Quantum Electron*, *8*, 362.
[9] Liu, T.-H., Iou, C.-Y., & Chen, C. H. (2003). *Appl. Phys. Lett.*, *83*, 5241.
[10] Li, G. & Shinar, J. (2003). *Appl. Phys. Lett.*, *83*, 5359.
[11] Choong, V. E., Shi, S., Curless, J., Shieh, C.-L., Lee, H.-C., Shen, J., & Yang, J. (1999). *Appl. Phys. Lett.*, *75*, 172.
[12] Chwang, A. B., Kwong, R. C., & Brown, J. J. (2002). *Appl. Phys. Lett.*, *80*, 725.
[13] Chen, C.-W., Cho, T.-Y., Wu, C.-C., Yu, H.-L., & Luh, T.-Y. (2002). *Appl. Phys. Lett.*, *81*, 1570.
[14] Qiu, Y., Gao, Y., Wang, L., Wei, P., Duan, L., Zhang, D., & Dong, G. (2002). *Appl. Phys. Lett.*, *81*, 3540.
[15] Coe, S., Woo, W.-K., Bawendi, M., & Bulović, V. (2002). *Nature*, *420*, 800.
[16] Sun, J. X., Zhu, X. L., Peng, H. J., Wong, M., & Kwok, H. S. (2005). *Appl. Phys. Lett.*, *87*, 93504.
[17] Ma, C., Zhang, B., Liang, Z., Xie, P., Wang, X., Zhang, B., Cao, Y., Jiang, X., & Zhang, Z. (2002). *J. Mater. Chem.*, *12*, 1671.
[18] Nalwa, H. S. & Rohwer, L. S. (ed), (2003). *Handbook of Luminescence, Display Materials, and Devices*, American Scientific Publishers: California, Vol. 1.
[19] Lampert, M. A. (1956). *Phys. Rev.*, *103*, 1648.
[20] Yamamoto, H., Kasajima, H., Yokoyama, W., Sasabe, H., & Adachi, C. (2005). *Appl. Phys. Lett.*, *86*, 83502.
[21] Brűtting, W., Berleb, S., & Műckl, A. G. (2001). *Org. Electron.*, *2,* 1.